Correlation between Wetting Properties and the Susceptibility to Wear of Rotary Shaft Sealing Systems

Philipp Fricker, Matthias Baumann, Frank Bauer

Modern lubricants (e.g. polyglycols, esters) cause problems when sealed with rotary shaft seals. The wear of rotary shaft seals strongly depends on the wetting properties of the respective friction partners. The paper shows, how the susceptibility to wear of rotary shaft sealing systems can be estimated by a combined consideration of the wetting properties of the sealing components, the lubricants viscosity and the pumping rate of the sealing system. Investigations were carried out using polished steel counter faces made from eight different alloys, together with FKM rotary shaft seals and eleven chemically different lubricants (mineral oils, polyglycols, poly-α-olefins, esters and silicone oils).

1 Introduction

Rotary shaft seals prevent the exchange of fluids between functional areas. This function must be guaranteed permanently or at least in the long term and is achieved by an active back-pumping mechanism, which is able to pump lubricant from the air side to the fluid side. An overview of the principles and hypotheses is given by Bauer [1]. Wear – which progresses over the operating period – at some point leads to the failure of the sealing system. The consequences range from damage to one’s image, to environmental damage, to economic damage due to the unavailability of machines and plants. So far, the suitability of the elastomer-counter face-fluid-compatibility can only be determined with practical tests after trial and error.

Wear occurs on all components of the rotary shaft sealing system, shown in Figure 1. In the case of the rotary shaft seal, it is mainly the sealing edge that is exposed to wear. This is characterized by the contact width. Wear, that takes place on the counter face, forms a circumferential groove. This wear is referred to as "wear track". An excessive wear interferes with the function of the rotary lip seal and ultimately leads to unwanted leakage.

During operation, a complete hydrodynamic lubricant film is formed between the rotary shaft seal and the counter face. According to Ott [2] fluid friction is assumed to be predominant. Therefore, rotary shaft seals should hardly wear at all if the speed is high enough and the lubricant supply is sufficient. For particle-free mineral oils this assumption is largely correct. However, chemically different lubricants (polyglycols, poly-α-olefins, esters), often deviate from this assumption. So far, the suitability of the elastomer-counter face fluid compatibility can only be determined with practical tests after trial and error, a time and cost-intensive procedure.

For this paper, wear test on 98 different rotary shaft sealing systems (polished shafts made out of eight different steel alloys, rotary shaft seals made of 75FKM585 and eleven chemically different lubricants: two mineral oil, four polyglycols, two poly-α-olefins, two esters and one silicone oil) were carried out and the system pumping rates were measured. For each component the relevant material and wetting properties were determined. It is shown how wear on rotary shaft sealing systems is related to the wetting properties of the system components. Furthermore, it is shown how the wear behavior of sealing systems can be estimated on the basis of wetting measurements of the individual sealing components used. In addition, a correlation model is introduced, which is able to predict the wear of the sealing system by the system pumping rate and a combined consideration of system spreading coefficient S_{SSYS}, the surface tension of the sealing counter face σ_{CF} and the lubricants viscosity η. The model allows users and manufacturers of rotary shaft sealing systems to estimate the wear of different sealing systems early in the design process. Thus, material pairings that are prone to wear can be avoided without having to perform numerous time-consuming and costly wear tests. This helps significantly to accelerate the approval process of rotary shaft sealing systems and to increase their service life.

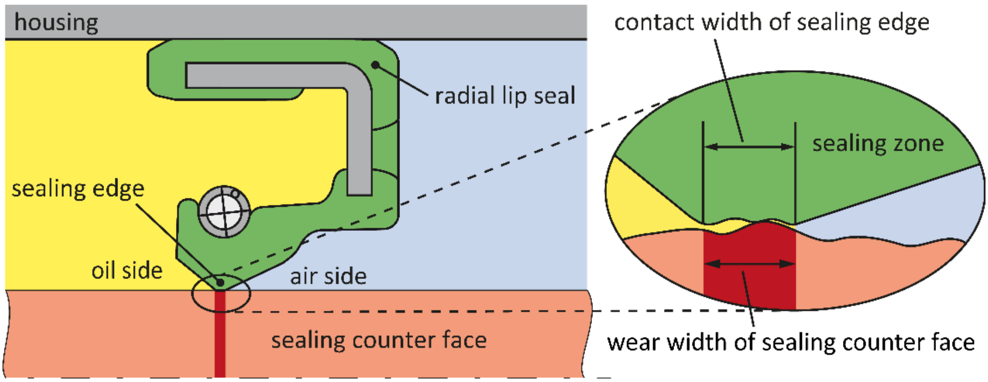

Figure 1: Installed rotary shaft sealing system [1]

2 State of the Art

This chapter gives an overview of the mathematical principals for calculating wetting properties in general and their transfer to rotary shaft sealing systems.

2.1 Interfacial Tension

An interface is created when two substances or phases come into contact. In the contact zone, intermolecular forces act, which cause an interaction between the substances or phases involved. According to Dörfler [3], these interactions are called interfacial tension. The interfacial tension σ_{ab} can simply be seen as an attraction force between the substances a and b in contact and can be divided in two partitions. One is an inward force on the surface molecules causing the liquid to contract. Second is a tangential force parallel to the surface of the liquid. This tangential force is generally referred to as the surface tension. According to Fowkes [4], the surface tension of each material is composed of a disperse component σ_d and a polar component σ_p. This is shown in Equation (1).

$$\sigma = \sigma_d + \sigma_p \tag{1}$$

According to Owens and Wendt [5], considering the geometric mean of the surface tensions σ_a and σ_b, the interfacial tension σ_{ab} can be determined by Equation (2)

$$\sigma_{ab} = \sigma_a + \sigma_b - 2\sqrt{\sigma_a^d \cdot \sigma_b^d} - 2\sqrt{\sigma_a^p \cdot \sigma_b^p} \tag{2}$$

Rabel [6] transformed Equation (2) to straight line form. Thus, the disperse and polar components of the surface tension of a solid σ_s could be determined for the first time by conducting two measurements with different measuring liquids using the sessile drop method. Kaelble [7] substituted the interfacial tension σ_{ab} with the work of adhesion W_a and obtained Equation (3). This allows the work of adhesion between a solid s and a liquid l to be calculated mathematically directly from the corresponding surface tensions σ_s and σ_l.

$$W_a = 2\left(\sqrt{\sigma_s^d} \cdot \sqrt{\sigma_l^d} + \sqrt{\sigma_s^p} \cdot \sqrt{\sigma_l^p}\right) \tag{3}$$

The calculation method is standardized in DIN 55660-2 [8] and is abbreviated OWRK. For determining the work of adhesion, Wu [9] proposes the harmonic mean, defined in Equation (4), instead of the geometric mean. He investigated polymer melts that did not mix with each other. The interfacial tension σ_{ab} could be measured directly. Thereby he noticed deviations from the OWRK calculation method.

$$\sigma_{ab} = \sigma_a + \sigma_b - 2\frac{2 \cdot \sigma_a^d \cdot \sigma_b^d}{\sigma_a^d + \sigma_b^d} - 2\frac{2 \cdot \sigma_a^p \cdot \sigma_b^p}{\sigma_a^p + \sigma_b^p} \tag{4}$$

The work of adhesion results in Equation (5).

$$W_a = 2\left(\frac{2 \cdot \sigma_a^d \cdot \sigma_b^d}{\sigma_a^d + \sigma_b^d} + \frac{2 \cdot \sigma_a^p \cdot \sigma_b^p}{\sigma_a^p + \sigma_b^p}\right) \tag{5}$$

The calculation method according to Wu is also standardized in DIN 55660-2 [8] and is recommended for low-energy surfaces with $\sigma < 20\,mN/m$.

2.2 Spreading Coefficient

Harkins and Feldman [10] introduced a measure for the wettability of solid surfaces by liquids. They defined the spreading coefficient S as the difference between the work of adhesion W_a and the work of cohesion W_c (the work of cohesion can be described as the bound energy between two surfaces of the same liquid). The work of cohesion is defined in Equation (6) as double the surface tension of the regarded liquid.

$$W_c = 2 \cdot \sigma_l \tag{6}$$

With the work of cohesion, the spreading coefficient S can be calculated using Equation (7).

$$S = W_a - W_c \tag{7}$$

Regarding the sealing gap, the lubricant interacts with a metal surface, the sealing counter face, as well as the elastomer surface of the sealing edge. To take this into account, the spreading coefficients for the two different solid surfaces must be considered in combination. For this purpose, we [11] introduced the approach of a system spreading coefficient S_{SSYS} as an addition of the two spreading coefficients S_{CF} and S_{SE} given in Equation (8). For spreading coefficients $S > 0$ Harkins and Feldman [10] assume complete wetting. For spreading coefficients $S < 0$ incomplete wetting occurs.

$$S_{SSYS} = S_{CF} + S_{SE} \tag{8}$$

3 Methods

This chapter introduces the methods for measuring the surface tension and gives an overview over the different sealing components used.

3.1 Measuring Instruments

3.1.1 Bubble Pressure Tensiometer

A bubble pressure tensiometer SITA SCIENCE LINE T60 was used to determine the surface tension of the liquids. The measuring principle is based on the Young-Laplace equation. A dried air stream is blown into the liquid through a capillary. Gas bubbles form at the tip, whose surface becomes more and more curved as the volume increases. Simultaneously the bubble radius decreases. From bubble formation to bubble detachment, the bubble pressure passes a characteristic pressure curve from which the surface tension of the surrounding liquid is calculated. The maximum pressure is reached at the smallest bubble radius. As the process progresses, the bubble radius increases rapidly and the bubble pressure drops, causing it to detach. The surface energy σ_l of the liquid is determined from the measured maximum pressure and the known capillary diameter.

3.1.2 Sessile Drop Method

A DataPhysics OCA20 contact angle measurement system was used to determine the surface tension of the solids. Drops of at least two different test liquids are successively deposited on the solid. In the static state the contour of the drop is determined. The contact angle is calculated by applying tangents to the drop contour at the two intersections with the base line (common phase boundary between drop and substrate). With the help of the contact angle, the disperse and polar fractions of the surface tension of the substrate can be determined mathematically according to OWRK and WU. The calculation methods are standardized in DIN 55660-2 [8].

3.1.3 Pendant Drop Method

A DataPhysics OCA20 contact angle measurement system was used to determine the polar and disperse fraction of the surface tension of liquids. A needle creates a pendant drop of a reference liquid in the liquid to be tested. According to the Young-Laplace equation, the characteristic shape of the pendant drop results in an interfacial tension between the tested liquid and the reference liquid. Together with the known surface tension of the reference liquid and the test liquid, the disperse fraction of the surface energy can be determined mathematically according to OWRK or WU. The calculation methods are standardized in DIN 55660-4 [12].

3.1.4 Tactile Surface Measurement

A tactile Hommel T8000 measurement instrument was used to measure the length and the depth of the wear track on the shaft counter faces after each test run. For this purpose, the shaft is clamped in a chuck. The texture of the surface and its roughness are measured by means of an axially movable stylus.

3.2 Test Parts

3.2.1 Shaft Materials

Polished shafts, made out of eight different steel alloys with an $80\ mm$ outer diameter, were used as shaft counter faces. Even though the surface finish of these polished counter faces differs from plunge-ground ones, used in the most applications, they offer advantages when investigating the influence of the wetting properties on the wear of different sealing components. Hydrodynamic effects induced by surface structures can be kept low. Directional structures, which create a fluid transport in axial direction under rotation of the shaft, so-called lead, are avoided. In addition, the counter faces of the used shafts have the same roughness characteristics as far as possible. The measurement of the surface tension can be carried out directly on the counter faces without having to use specially manufactured test specimens. The hardness of the counter faces ranged from $44.7\ HRC$ to $61.9\ HRC$. The surface roughness was between $R_z = 0.036\ \mu m$ and $0.161\ \mu m$. The exact values for each shaft and alloy can be found in [11].

3.2.2 Elastomer Material

For the test bench investigations, rotary lip seals of the type BAUM5X7 made of 75FKM585 with a sealing diameter of $80\ mm$ were used (material properties by Freudenberg [13]). These are standard type rotary lip seals according to DIN 3760/61 [14, 15] with an outer elastomer sleeve and a spring-loaded fluorine rubber sealing lip for high thermal and chemical requirements. These rotary lip seals are largely inert to the lubricants used.

3.2.3 Lubricants

For this paper, investigations on eleven different lubricants were performed, consisting of five different base oils (mineral oils, poly-α-olefins, polyglycols, esters and silicone oils). This includes lubricants that don't contain additives as well as lubricants that do. Table 1 lists the lubricants used, In the following, the respective lubricants are designated with the abbreviation given.

Table 1: Lubricants. viscosity at $T = 60\ °C$ [11]

Manufacturer	Product Name	Base Oil	Additives	Viscosity [mPAS]
FVA	FVA2	Mineral Oil	None	12.4
FVA	FVA3	Mineral Oil	None	33.2
FVA	PAO2	Poly-α-Olefin	None	25.2
FVA	PAO3	Poly-α-Olefin	None	77.8
FVA	PG1	Polyglycol	None	38.0
FVA	PG3	Polyglycol	None	111.4
Mobile	Glygoyle 22	Polyglycol	Yes	73.4
Anonymized	Anonymized	Polyglycol	Yes	77.1
Fuchs	Cassida GLE-150	Ester	Yes	50.4
Anonymized	Anonymized	Ester	Yes	55.9
OKS	1010/1	Silicone Oil	None	51.2

3.2.4 Pumping Rate Tests

To quantify how the different lubricants effect the active back-pumping rate of a rotary shaft sealing system, experimental pumping rate tests were carried out. These pumping rate tests can give an indication on the leak tightness of rotary shaft sealing systems [16, 17]. For these test, the rotary shaft seals have been mounted inversely (the oil sump was located on the air side only) and the test chamber was filled with lubricant up to the center of the shaft. The test duration was $10\ h$ and the oil sump temperature $40\ °C$. The revolution speed was a constant $1000\ rpm$, which corresponds to a shaft speed of $4.2\ ms^{-1}$. For each combination three tests were carried out. Static and dynamic eccentricity has been measured before each test run and kept below $20\ \mu m$.

3.2.5 Wear Tests

The wear tests were carried out on the institute's 12-cell test bench [18]. The test duration was $100\ h$ and the oil sump temperature $40\ °C$. The revolution speed was a constant $1000\ rpm$, which corresponds to a shaft speed of $4.2\ ms^{-1}$. For each combination, three tests were carried out. Static and dynamic eccentricity has been measured before each test run and kept below $20\ \mu m$. Leakage only occurred in conjunction with the silicone oil OKS 1010/1 with a total amount of $< 1\ g$ over the test duration of $100\ h$.

4 Results

The results presented in this work are based on the analyses conducted in the AiF research project “Welleneinlauf” [11].

4.1 Material Values

4.1.1 Surface Tension of Shaft and Elastomer Materials

The three measuring liquids ethylene glycol, 1-bromo-naphthalene and thiodiglycol were used to determine the surface tensions of the shaft counter faces and the elastomer. The measurements were carried out according to DIN55660-2 [8]. The calculated values for the surface tensions are listed in Table 2.

Table 2: Surface tension of shaft and elastomer material $T = 20\ °C$ in $[{}^{mN}/_{m}]$.

	100Cr6	C45	16MnCr5	X39CrMo17	42CrMo4	C60	30CrNiMo8	X20Cr13	75FKM585
σ	38.1	34.0	34.6	40.8	38.2	38.0	39.2	39.8	19.3
σ_d	21.9	24.9	22.4	16.7	28.2	24.2	20.2	20.7	12.6
σ_p	16.3	9.2	12.2	24.0	10.0	13.8	19.0	19.1	6.7

4.1.2 Surface Tension of Lubricants

The pendant drop method was used to determine the disperse and polar fractions of the surface tension. Perfluoro octane was used as a reference liquid. The measurements were carried out according to DIN55660-4 [12]. The disperse and polar fraction of the surface tension were determined using to the method of OWRK according to DIN55660-3 [19]. As a reference liquid, purely disperse perfluoro octane ($\sigma_p = 14.0\ mN/m$, Ström [20]) has been used. The values are shown in Table 3.

Table 3: Surface tension of lubricants $T = 20\ °C$ in $[{}^{mN}/_{m}]$.

	FVA2	FVA3	PAO2	PAO3	PG1	PG3	MGP	PX	FCE	EX	OSO
σ	32.1	32.8	26.8	31.9	36.4	39.8	33.1	33.8	30.7	32.5	21.1
σ_d	24.5	24.8	17.9	23.3	24.3	25.2	26.1	21.24	25.0	23.6	16.0
σ_p	7.6	8.0	8.8	8.5	12.1	14.6	7.0	12.56	5.7	8.9	5.1

The lowest surface tension can be found for the silicon oil OSO. Polyglycols on the other hand show the highest surface tension. This gives an indication of why increased wear on the sealing system is often observed when sealing polyglycols. A higher surface tension of the lubricant leads to an increase in the work of cohesion. It is assumed that this has a negative influence on the wetting properties in the sealing gap, which can ultimately increase wear. Within a considered base oil class, the surface tension increases with an increase in viscosity.

4.1.3 System Spreading Coefficient

The tendency of a liquid to spread in the sealing gap can be described by the spreading coefficient S_{SSYS}. Mathematically, it is described by Equation (8). Based on DIN55660-2 [8], the spreading coefficients of all lubricant on the counter faces and 75FKM585 were calculated with the work of adhesion according to OWRK. The resulting system spreading coefficients S_{SSYS} are listed in Table 4.

Table 4: System spreading coefficients S_{SSYS} for $T = 20\ °C$ in $\left[{}^{mN}/_{m}\right]$.

	FVA2	FVA3	PAO2	PAO3	PG1	PG3	MGP	PX	FCE	EX	OSO
100Cr6	-10.4	-11.9	2.0	-9.3	-18.5	-26.1	-13.3	-12.4	-8.9	-10.5	11.3
C45	-12.8	-14.5	-1.4	-12.2	-22.4	-30.6	-15.5	-16.7	-10.6	-13.5	9.3
16MnCr5	-12.8	-14.4	-0.8	-12.0	-21.7	-29.6	-15.6	-15.8	-10.9	-13.2	9.3
X39CrMo17	-11.4	-12.8	2.2	-9.9	-18.2	-25.3	-14.7	-11.7	-10.6	-11.0	10.6
42CrMo4	-8.9	-10.5	2.1	-8.3	-18.3	-26.4	-11.5	-12.8	-6.7	-9.6	12.4
C60	-9.7	-11.2	2.2	-8.8	-18.3	-26.0	-12.5	-12.4	-8.0	-10.0	11.8
30CrNiMo8	-10.3	-11.8	2.4	-9.2	-18.0	-25.4	-13.4	-11.8	-9.1	-10.3	11.4
X20Cr13	-9.7	-11.2	2.9	-8.6	-17.4	-24.7	-12.8	-11.2	-8.5	-9.7	11.8

The highest system spreading coefficient S_{SSYS} can be found for the silicon oil. Polyglycols on the other hand show the lowest system spreading coefficients. It is assumed that a lower system spreading coefficient leads to less sufficient lubrication in the sealing gap and thus generates more wear on the sealing system [11, 21].

4.2 Pumping Rate

To determine the pumping rate of the different sealing systems, each combination was tested three times and evaluated according to [11]. The mean values of the measured pumping rates are listed in Table 5.

Table 5: Pumping rate of lubricants in $\left[{}^{g}/_{h}\right]$.

	FVA2	FVA3	PAO2	PAO3	PG1	PG3	MGP	PX	FCE	EX	OSO
100Cr6	0.98	1.41	2.01	2.85	2.03	3.12	3.01	2.69	1.84	3.42	1.48
C45	1.46	2.16	1.91	2.32	2.60	4.81	2.24	3.83	2.08	2.33	1.37
16MnCr5	1.11	1.65	2.18	2.71	2.63	3.02	2.99	2.81	2.07	3.53	1.77
X39CrMo17	0.56	1.31	1.57	1.68	1.66	2.06	1.92	1.78	1.74	2.83	1.33
42CrMo4	1.31	1.54	1.25	2.19	1.64	2.37	3.04	3.32	1.74	3.28	1.36
C60	1.20	2.26	1.96	2.90	2.01	3.54	3.05	3.31	1.76	3.33	1.35
30CrNiMo8	1.25	1.77	2.08	2.11	1.76	3.07	2.20	2.50	2.00	3.36	1.30
X20Cr13	0.91	1.24	2.07	2.13	1.90	2.60	2.50	2.20	1.60	2.80	1.40

In order to classify the determined pumping rates, these can be compared to the values from Bekgulyan [17]. For his pumping rate measurements, he used plunge-ground counter faces instead of polished ones and tested them in combination with the lubricants FVA3, PAO3 and PG3. using the same type of rotary lip seals. The pumping rates shown in *Table 5* are about 20% lower than Bekgulyans. The lower pumping rates using polished counter faces are in line with the research of Remppis [16]. With decreasing surface roughness, he observed a decrease of the pumping rate.

4.3 Wear track depth

To determine the depth of the shaft wear tracks, the shafts were measured according to [11, 22]. The wear track depth h_d for the different sealing systems are listed in Table 6 as an average of the three test runs of each combination. The individual values for each test run can be found in [11].

Table 6: Average wear track depth of three test runs per combination $[\mu m]$.

	FVA2	FVA3	PAO2	PAO3	PG1	PG3	MGP	PX	FCE	EX	OSO
100Cr6	0.00	4.57	2.16	4.89	8.84	10.70	3.60	4.70	0.29	17.45	0.00
C45	0.00	4.14	6.12	10.67	9.72	25.66	24.97	9.85	11.86	14.99	0.00
16MnCr5	0.00	0.00	3.24	3.75	4.43	26.67	25.13	15.02	20.33	31.02	0.00
X39CrMo17	0.00	0.00	0.00	0.09	1.49	2.37	2.78	4.60	0.00	7.00	0.00
42CrMo4	0.00	0.85	0.00	4.42	9.32	8.38	24.95	9.04	12.65	18.22	0.00
C60	0.00	8.64	0.00	7.89	5.54	13.77	12.30	16.70	5.48	19.53	0.00
30CrNiMo8	0.00	0.00	0.00	6.89	5.52	10.37	10.46	10.57	7.51	13.24	0.00
X20Cr13	0.00	2.30	0.00	4.02	0.00	7.25	8.75	6.43	4.34	7.61	0.00

4.4 Contact width

To determine the contact width l_c of the sealing edge, the radial lip seals were photographed using an IMA-Sealobserver® in conjunction with a digital microscope. The photographs were evenly distributed around the entire circumference and evaluated according to [11]. The detected contact widths of the combinations are listed in Table 7.

Table 7: Average contact width of three test runs per combination $[mm]$.

	FVA2	FVA3	PAO2	PAO3	PG1	PG3	MGP	PX	FCE	EX	OSO
100Cr6	0.15	0.29	0.17	0.28	0.34	0.27	0.31	0.37	0.25	0.46	0.17
C45	0.19	0.25	0.23	0.32	0.36	0.36	0.61	0.50	0.50	0.52	0.16
16MnCr5	0.19	0.22	0.25	0.24	0.26	0.54	0.54	0.50	0.50	0.56	0.19
X39CrMo17	0.18	0.18	0.20	0.21	0.24	0.26	0.28	0.43	0.24	0.34	0.19
42CrMo4	0.20	0.21	0.19	0.26	0.28	0.33	0.57	0.33	0.49	0.39	0.16

C60	0.19	0.30	0.19	0.45	0.32	0.42	0.41	0.47	0.33	0.48	0.16
30CrNiMo8	0.26	0.24	0.20	0.45	0.34	0.28	0.29	0.39	0.30	0.41	0.17
X20Cr13	0.22	0.25	0.22	0.28	0.23	0.32	0.31	0.36	0.29	0.37	0.18

4.5 Correlation

The wear track depth h_d of the counter faces and the contact width l_c of the worn sealing edge are compared with each other in Figure 2. Across all the wear tests performed, a linear relationship with a correlation coefficient of $R = 0.88$ is obtained between the two parameters. Contact widths $l_c < 0.16\,mm$ could not be found in any of the wear tests carried out. Likewise, wear of the counter face was observed only in combination witch contact widths $l_c \geq 0.16\,mm$. For small contact widths $l_c < 0.16\,mm$, initial wear of the sealing edge is assumed, which is necessary to generate an active sealing mechanism and can therefore not be considered wear in the actual sense [1].

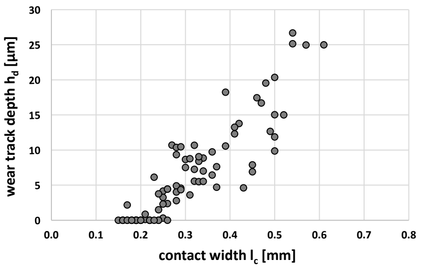

Figure 2: Relation between wear track depth h_d and contact width l_c

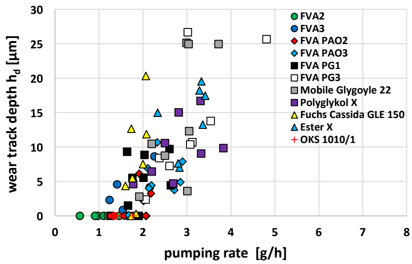

Figure 3: Influence of the pumping rate on the wear track depth h_d

Due to the linear correlation of the individual wear parameters of the counter face and the sealing edge, the wear track depth h_d of the counter face is used as a measure for the wear of the sealing system in the further course of this work.

In Figure 3, the wear track depth h_d of the counter faces and the pumping rates of the sealing systems are compared with each other. An increase in the pumping rate correlates to an increase in wear. Similar to the phenomenon of insufficient lubrication due to lead, described by Baumann [23], an increase in the pumping rate of the sealing system can lead to insufficient lubrication in the sealing contact. The consequence is an increase in solid contact between the counter face and sealing edge, which leads to an increased wear of the sealing components involved. From this point of view, it must be concluded that a particularly high pumping rate increases sealing reliability on the one hand, but at the same time the higher wear limits the service life. Figure 4 shows the wear track depth h_d of the sealing counter faces plotted against the system spread coefficient S_{SSYS}. The detected wear track depth h_d increases with a decreasing system spreading coefficients S_{SSYS} but the scattering is high within each lubricant.

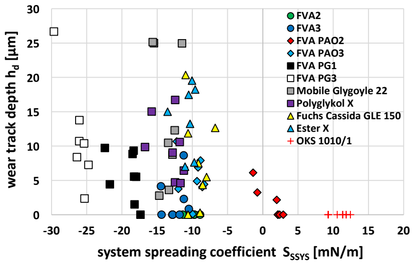

Figure 4: Influence of the system spreading coefficient S_{SSYS} on the wear track depth h_d

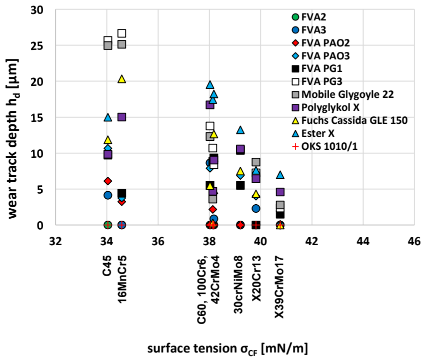

Figure 5: Influence of surface tension of the sealing counter face σ_{CF} on the wear track depth h_d

The scattering in Figure 4 can be explained by considering the surface tension σ_{CF} of the different alloys the sealing counter faces are made of, shown in Figure 5. A decrease in the determined wear track depth h_d with an increasing surface tension σ_{CF} becomes apparent. Particularly when comparatively low-energy counter faces made of C45 and 16MnCr5 are used, higher wear track depths occur in combination with polyglycol- and ester-based lubricants.

4.6 Correlation Model

Based on the parameters of a rotary shaft sealing system in chapter 4.4, a correlation model is developed, which can be used to estimate the wear that is expected during operation. Considering all 264 tests (88 combinations, three tests each) carried out so far, the pumping rate $\dot{m}_r$ of a rotary shaft sealing system can be used to calculate the wear track depth $h_{d,c}$ from Equation (9).

$$h_{d,c} = -7.86 + 6.649 \cdot \dot{m}_r \tag{9}$$

The values calculated according to Equation (9) are compared with the measured wear track depths h_d in Figure 6. The linear correlation coefficient is $R = 0.69$. 82 % of the calculated wear track depths $h_{d,c}$ show a deviation of $\leq 5\ \mu m$ to the detected values. With the help of Equation (10), the pumping rate $\dot{m}_{r,cal}$ can be calculated by the system spreading coefficient S_{SSYS}. To increase the accuracy of the correlation, the lubricant viscosity η and the surface tension of the counter face σ_{CF} are also considered.

$$\dot{m}_{r,cal} = 6{,}059 + 0{,}01731 \cdot \eta - 0{,}1307 \cdot \sigma_{CF} - 0{,}00636 \cdot S_{SSYS} \tag{10}$$

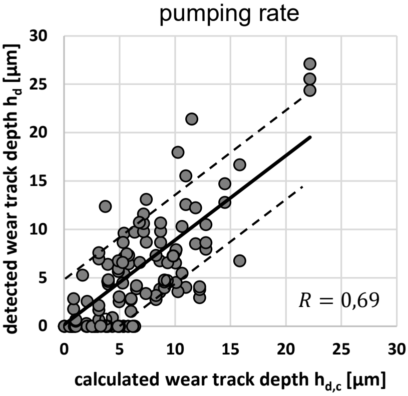

Figure 6: Model for estimating the wear on rotary shaft seal systems based on the system pumping rate $\dot{m}_r$

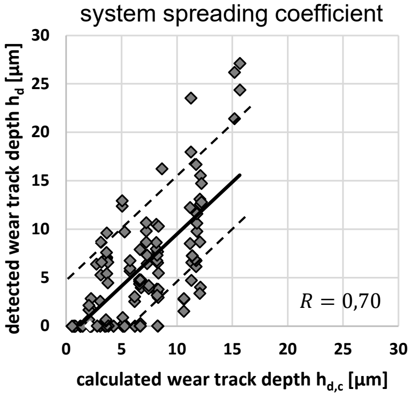

Figure 7: Model for estimating the wear on rotary shaft seal systems based on the system spreading coefficient S_{SSYS} [1]

The values calculated according to Equation (10) are compared with the measured wear track depths h_d in Figure 7. The linear correlation coefficient is $R = 0.70$. 87 % of the calculated wear track depths $h_{d,c}$ show a deviation of ≤ 5 µm to the detected values.

5 Summary and Conclusion

Modern lubricants, such as polyglycols and esters, cause problems when sealed with rotary shaft seals. Besides chemical incompatibility with the elastomer, increased wear and finally leakage can occur. The cause of these disadvantages compared to conventional, mineral oil-based lubricants is assumed to be in the wetting properties of the lubricants. Different sealing systems were investigated to examine this behavior. Combinations of polished steel counter faces made out of eight different alloys, rotary lip seals made of 75FKM585 and eleven chemically different lubricants were used.

Sealing systems with an increased pumping rate show increased wear of the sealing system. This can be explained by regarding the functional principles of rotary shaft sealing systems summarized in [1]. The lubricant, brought into the sealing gap by the rotary motion of the shaft counter face, is pumped back to the oil side by an active back-pumping mechanism. This active back pumping mechanism prevents leakage. While the lubricant is in the sealing gap, it causes the sealing edge to float. The sealing edge lifts off the counter face and thus reduces wear of the friction partners. If the system pumping rate is too high, more lubricant can potentially be brought back to the oil side than it is necessary for a sufficient lubrication of the sealing gap. Solid contact between the sealing edge and the counter face increases, which promotes increased wear. The wetting properties of the sealing components must also be included in this consideration. The ability of a lubricant to stay in the sealing gap is determined primarily by the system spreading coefficient. The higher the value, the stronger the lubricant bonds to the elastomer and the counter face. This increased bond ensures a sufficient lubricating film between the friction partners and thus contributes to a reduction in wear. Based on the pumping rate and the system spreading coefficient a correlation model is introduced which is able to describe the tribological behavior and to predict the expected wear during operation of different rotary shaft sealing systems.

Considering the previously discussed observations, it must be noted that the model presented in this paper is based on empirical data. Strictly speaking, it is only valid for the material combinations used here. In the future, it must be proven that it can be transferred to other rotary shaft sealing systems. Also, polished counter faces were used for all tests within this work. These deviate from plunge-ground counter faces which are mainly used in rotary shaft sealing systems. Schulz [24] showed that the different surface structure can have a significant influence on the hydrodynamics in sealing contact. Polished counter surfaces, on the other hand, do not exhibit significant surface structures. Therefore, it can be assumed that the correlations between the wetting properties and the wear on the polished shafts can be transferred to plunge-ground counter faces. However, it can be expected that these are less pronounced due to changes in hydrodynamics regarding the sealing gap. The results show for the first time that it is possible to identify suitable and coordinated oil-elastomer-counter face combinations before using costly and time-consuming wear tests.

To reduce wear, negative system spreading coefficients and high pumping rates can be used to identify and avoid critical material combinations early in the design process as far as possible. If other material combinations are not possible, further wear reducing strategies must be considered. Based on this work, a promising approach could be reducing the pumping rate of the sealing system.

6 Acknowledgements

The IGF project 20111 N/1 of the Forschungskuratorium Maschinenbau e.V. (FKM) was funded by the AiF as a support of the Industrielle Gemeinschaftsforschung (IGF, Industrial Collective Research) by the Federal Ministry for Economic Affairs and Energy (BMWi) on the basis of a decision by the German Bundestag.

Supported by:

Federal Ministry for Economic Affairs and Energy

on the basis of a decision by the German Bundestag

FKM Forschung im VDMA

7 Nomenclature

Variable	*Description*	*Unit*

h_d	Wear Track Depth	$[m]$
$h_{d,c}$	Calculated Wear Track Depth	$[m]$
l_c	Contact Width	$[m]$
$\dot{m}_t$	Pumping Rate	$[{}^{g}/_{h}]$
$\dot{m}_{t,cal}$	Calculated Pumping Rate	$[{}^{g}/_{h}]$
S	Spreading Coefficient	$[{}^{mN}/_{m}]$
S_{CF}	Spreading Coefficient of Sealing Counter Face	$[{}^{mN}/_{m}]$
S_{FKM}	Spreading Coefficient on 75FKM585	$[{}^{mN}/_{m}]$
S_{SE}	Spreading Coefficient of Sealing Edge	$[{}^{mN}/_{m}]$
S_{SSYS}	System Spreading Coefficient	$[{}^{mN}/_{m}]$
T	Temperature	$[°C]$
W_a	Work of Adhesion	$[{}^{mN}/_{m}]$
W_c	Work of Cohesion	$[{}^{mN}/_{m}]$
η	Viscosity	$[mPas]$
θ	Contact Angle	$[°]$
σ	Surface Tension	$[{}^{mN}/_{m}]$
σ_a	Surface Tension of Material a	$[{}^{mN}/_{m}]$
σ_b	Surface Tension of Material b	$[{}^{mN}/_{m}]$
σ_{ab}	Interfacial Tension	$[{}^{mN}/_{m}]$
σ_d	Surface Tension, Disperse Fraction	$[{}^{mN}/_{m}]$
σ_l	Surface Tension of a Liquid	$[{}^{mN}/_{m}]$
σ_p	Surface Tension, Polar Fraction	$[{}^{mN}/_{m}]$
σ_s	Surface Tension of a Solid	$[{}^{mN}/_{m}]$
ω	Angular velocity	$[rad \cdot s^{-1}]$

8 References

[1] **Bauer, F.:** *Federvorgespannte-Elastomer-Radial-Wellendichtungen. Grundlagen der Tribologie & Dichtungstechnik, Funktion und Schadensanalyse*, Wiesbaden, Heidelberg: Springer Vieweg, 2021, Springer Fachmedien Wiesbaden, - ISBN 978-3-658-32922-8.

[2] **Müller, H. K.; Ott, G.:** *Dichtwirkung von Radialwellendichtringen.* Erschienen in: *Tribologie.* Gleitlager, Mischreibung, Konstruktive Gestaltung. Band 6; Berlin, Heidelberg: Springer Verlag, 1983 - ISBN 3642522270.

[3] **Dörfler, H.-D.:** *Grenzflächen und kolloid-disperse Systeme. Physik und Chemie ; mit 579, zum Teil farbigen Abb. und 88 Tabellen*, Berlin: Springer, 2002, - ISBN 9783540425472.

[4] **Fowkes, F. M.:** *ATTRACTIVE FORCES AT INTERFACES*. Industrial & Engineering Chemistry. 1964, 56 (12), S. 40–52.

[5] **Owens, D. K.; Wendt, R. C.:** *Estimation of the surface free energy of polymers*. Journal of Applied Polymer Science. 1969, 13 (8), S. 1741–1747.

[6] **Rabel, W.:** *Einige Aspekte der Benetzungstheorie und ihre Anwendung auf die Untersuchung und Veränderung der Oberflächeneigenschaft von Polymeren.,* 1997, Farbe und Lack 77 (1971), NR. 10, S. 997–1005.

[7] **Kaelble, D. H.:** *Dispersion-Polar Surface Tension Properties of Organic Solids*. The Journal of Adhesion. 1970, 2 (2), S. 66–81.

[8] **DIN 55660-2, 2011:** *DIN 55660-2:2011-12, Beschichtungsstoffe_- Benetzbarkeit_- Teil_2: Bestimmung der freien Oberflächenenergie fester Oberflächen durch Messung des Kontaktwinkels*, Berlin: Beuth Verlag GmbH.

[9] **Wu, S.:** *Polar and Nonpolar Interactions in Adhesion*. The Journal of Adhesion. 1973, 5 (1), S. 39–55.

[10] **Harkins, W. D.; Feldman, A.:** *FILMS. THE SPREADING OF LIQUIDS AND THE SPREADING COEFFICIENT*. Journal of the American Chemical Society. 1922, 44 (12), S. 2665–2685.

[11] **Fricker, P.; Baumann, M.; Bauer, F.:** *Welleneinlauf. Einfluss der Schmierstoffbenetzung auf den Verschleiß der Gegenlauffläche bei Radial-Wellendichtungen*. Abschlussbericht FKM Vorhaben Nr. 612, IGF-Nr: 20111, Frankfurt am Main: FKM, 2021, Forschungskuratorium Maschinenbau e.V. (FKM).

[12] **DIN 55660-4, 2012:** *DIN 55660-4:2012-04, Beschichtungsstoffe_- Benetzbarkeit_- Teil_4: Bestimmung des polaren und dispersen Anteils der Oberflächenspannung von Flüssigkeiten aus einer Grenzflächenspannung*, Berlin: Beuth Verlag GmbH.

[13] **Freudenberg Forschungsdienste KG:** *Elastomere Werkstoffe,* 2001.

[14] **Deutsches Institut für Normung e.V.:** DIN 3760: *Radial-Wellendichtringe*, Berlin. September 1996.

[15] **DIN-Normenausschuss Maschinenbau Fachbereich Fluidtechnik:** DIN 3761: *Radial-Wellendichtringe für den Maschinenbau (NA 060-36-74 AA).* 2018.

[16] **Remppis, M.:** *Untersuchungen zum Förderverhalten von Dichtsystemen mit Radial-Wellendichtringen aus Elastomer*. Dissertation, 2016, Universität Stuttgart, Institut für Maschinenelemente, - ISBN 978-3-936100-68-6.

[17] **Bekgulyan, S.; Bauer, F.; Haas, W.:** *Berechenbare Dichtgüte II. Rechnerische Abschätzung der Dichtgüte von Radial-Wellendichtungen durch Kenntnis der Systemparametereinflüsse II*. Abschlussbericht FVA Vorhaben Nr. 617 II, IGF-Nr. 17938 N/1, Frankfurt am Main: FVA, 2017, Forschungsvereinigung Antriebstechnik e.V. (FVA).

[18] **Universität Stuttgart, Institut für Maschinenelemente:** *Wellendichtungen 24-Zellen-Dauerlaufprüfstand.* Universität Stuttgart, Institut für Maschinenelemente (Hrsg.), IMA-TechSheet, V1, #101010, Stuttgart, URL: https://www.ima.uni-stuttgart.de/dokumente/forschung/dichtungstechnik/einrichtungen/101010.pdf.

[19] **DIN 55660-3, 2011:** *DIN 55660-3:2011-12, Beschichtungsstoffe_- Benetzbarkeit_- Teil_3: Bestimmung der Oberflächenspannung von Flüssigkeiten mit der Methode des hängenden Tropfens*, Berlin: Beuth Verlag GmbH.

[20] **Ström, G.; Fredriksson, M.; Stenius, P.:** *Contact angles, work of adhesion, and interfacial tensions at a dissolving Hydrocarbon surface*. Journal of Colloid and Interface Science. 1987, 119 (2), S. 352–361.

[21] **Schuler, P.:** *Einfluss von Grenzflächeneffekten auf den Dichtmechanismus der Radial-Wellendichtung*. Dissertation, 2014, Universität Stuttgart, Institut für Maschinenelemente, - ISBN 978-3-936100-54-9.

[22] **Fricker, P.; Baumann, M.; Bauer, F.:** *How different lubricants affect the wear of steel counterfaces in radial lip sealing systems*. Wear. 2021 (203897).

[23] **Baumann, M.:** *Abdichtung drallbehafteter Dichtungsgegenlaufflächen - Messung, Analyse, Bewertung und Grenzen*. Dissertation, 2017, Universität Stuttgart, Institut für Maschinenelemente, - ISBN 978-3-936100-69-3.

[24] **Schulz, M.; Baumann, M.; Bauer, F.; Haas, W.:** *Influence of different shaft surface finishes on the tribological and functional behaviour of radial shaft seals.* 11th International Fluid Power Conference, Aachen, 19.-21.03.2018, 2018, S. 86–98 - ISBN 978-3-95886-215-9.

9 Authors

University of Stuttgart. Institute of Machine Components (IMA)

Pfaffenwaldring 9. 70569 Stuttgart. Germany:

Philipp Fricker. M. Sc. ORCID 0000-0002-2076-0408. philipp.fricker@web.de

Dr.-Ing. Matthias Baumann. ORCID 0000-0002-1962-5153. matthias.baumann@ima.uni-stuttgart.de

PD Dr.-Ing. Frank Bauer. ORCID 0000-0001-7799-7628. frank.bauer@ima.uni-stuttgart.de